ELSEVIER

Biophysical Chemistry 94 (2001) 75–85

Biophysical Chemistry

www.elsevier.com/locate/bpc

Phase-fluorometry study on dielectric relaxation of acrylodan-labeled human serum albumin

Andrea Buzády[a,b,*], János Erostyák[a,c], Béla Somogyi[b,d]

[a] *Department of Experimental Physics, Institute of Physics, University of Pécs, H-7624 Pécs, Ifjúság u. 6., Hungary*
[b] *Department of Biophysics, University of Pécs, H-7625 Pécs, Szigeti út 12., Hungary*
[c] *Jobin-Yvon Molecular Luminescence Reference Laboratory, University of Pécs, H-7624 Pécs, Ifjúság u. 6., Hungary*
[d] *Research Group for Fluorescence Spectroscopy, Office for Academy Research Groups Attached to Universities and Other Institutions, H-7625 Pécs, Szigeti út 12., Hungary*

Received 16 May 2001; received in revised form 13 August 2001; accepted 14 August 2001

Abstract

Dielectric relaxation (DR) of acrylodan-labeled human serum albumin (HSA/AC) was studied by phase-fluorometry. A non-monoexponential behavior of both the total fluorescence — and the DR decays has been found. The protein environment of the fluorescent marker shows DR times ranging from the pico to nanosecond timescale. In fluorescence emission decays measured on the red side of the fluorescence spectrum a time constant (< 10 ps) affected by a negative preexponential was found supporting the existence of DR of the excited states. © 2001 Elsevier Science B.V. All rights reserved.

Keywords: Dielectric relaxation; Acrylodan; Human serum albumin; Phase-fluorometry; Time-emission matrix

1. Introduction

The time-dependent Stokes shift (TDSS) of fluorophores provides useful information about dielectric relaxation (DR) phenomena [1–4]. Protein dynamics are generally studied through observation of fluorescence emission of either an intrinsic fluorophore group (i.e. tryptophan) [5–14] or a polarity-sensitive probe attached to the protein [15–18]. The fluorescence emission of a protein reflects both the ground state heterogeneity and the presence of DR. Both of these phenomena results in fluorescence decays which can be described with distributed relaxation rates. The ground-state heterogeneity is generally associated

* Corresponding author. Tel.: +36-72-503600/4488; fax: +36-72-501571.
E-mail address: buzady@fizika.ttk.pte.hu (A. Buzády).

PII: S0301-4622(01)00212-5

with the existence of different conformer states. DR also results in TDSS of fluorescence emission, generally towards the red (longer wavelength) direction of the spectrum.

Briefly, TDSS can occur when the dipole moment of the fluorophore in the excited state differs from that in the ground state. Right after excitation, the fluorophore is out of equilibrium with its surroundings and an excited state relaxation starts. This relaxation appears in the fluorescence emission as a time-dependent red shift, which serves as an instantaneous measure of energy gap between the ground and excited electronic states. In proteins, where a fluorophore is surrounded by a complex environment, the DR may have both faster and slower components. The former one is due to the relaxation of solvent molecules or the closest groups, the latter one is due to the longer scale motions of the protein.

Unquestionable evidence of the presence of DR is the existence of time constants with negative preexponentials in the exponential series describing the fluorescence decay. The ground state heterogeneity yields fluorescence decays associated with distributed fluorescence decay rates, but never with negative preexponentials.

Human serum albumin (HSA) is the principal carrier of fatty acids in the blood and the details of ligand binding to HSA has been studied for decades. There are three structurally homologous domains that repeat in HSA [19]. Each domain is formed by two smaller subdomains. In this work, we have focused on the dynamics surrounding the Cys-34 group of the HSA located in domain I (Fig. 1). For this purpose a site-selective fluorescent probe, 6-acryloyl-2-dimethyl-aminonaphtalene (Acrylodan, AC) [20] was used. It is thiol-selective thus it reacts only with the one free thiol at Cys-34. Fluorescence emission of AC is extremely sensitive to the environment of the probe and is affected by both the surrounding protein matrix and the solvent molecules. Both fluorescence emission and DR has components in the ps–ns timescales, which are detectable with our phase-fluorometer. We investigated the influence of solvent constituents and temperature on the decays of both the fluorescence emission and DR.

Earlier, AC was used to label different proteins. Among others, the HSA/AC system was also studied by different groups. Bright and coworkers focused on the dynamics of bovine and human serum albumin after different preparations [21–24]. Quenching experiments revealed the accessibility of AC in the AC-labeled serum albumins during denaturation [25,26]. The most frequently used methods are the steady-state fluorescence (SSF), time-resolved fluorescence (TRF) and total internal reflection fluorescence (TIRF) [27].

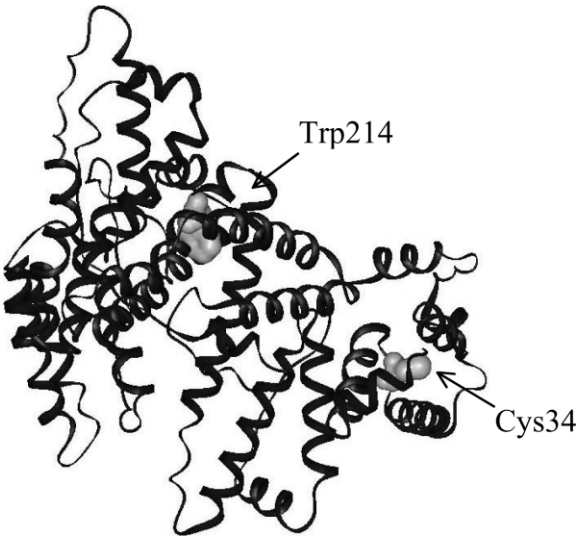

Fig. 1. Positions of tryptophan and cysteine are shown in three-dimensional structure of HSA. Picture was created by WebLab ViewerLite program based on a Protein Data Bank file.

Our aim was to determine the origin of spectral shift of the fluorescence emission and probe the dynamics surrounding the AC within the labeled, native HSA. We used steady-state and time-resolved fluorescence techniques to investigate HSA/AC.

2. Materials and methods

2.1. Materials

HSA was obtained from Sigma and used without further purification. AC was purchased from

Molecular Probes. Glycerol and glycogen were obtained from Sigma.

The labeling of HSA was done using Wang's method [23] with minor modifications. The protein solution containing 7.24×10^{-5} M HSA was prepared in 0.1 M sodium phosphate buffer of pH 7.0. Sufficient AC (the molar ratio was 1:1) was freshly dissolved in 50 μl DMF and added to the HSA/buffer with gentle stirring. This mixture was allowed to react for 6 h at room temperature. Then it was loaded into a dialysis bag and dialyzed at 4°C against 0.1 M sodium phosphate buffer pH 7.0. After 4 days with continuos changing of the buffer every 12 h to remove any residual free AC the HSA/AC solution was passed trough a Sephadex G-25 column.

After labeling of HSA, glycerol was added to the HSA/AC solution in a 10% ratio (w/w) of glycerol/buffer in some experiments. At this low concentration of glycerol no denaturation occurs.

In time-resolved measurements the reference solution was glycogen in water or in glycerol/water freshly prepared.

2.2. Steady state fluorescence and phase-fluorometry measurements

Both steady state fluorescence and phase-fluorometry measurements were carried out by a Jobin–Yvon Fluorolog τ3 fluorometer [14]. The steady state measurements were performed by the single-photon counting system mode. The spectral resolution of the steady state spectra was 1 nm.

In phase-fluorometry mode, emission was collected for frequencies in the range of 10–200 MHz, measuring at least 12 different modulation frequencies distributed equidistantly in frequency space.

In these measurements, the spectral resolution of the monochromators were set at: excitation monochromator, 2 nm; emission monochromator, 20 nm.

For both steady state and time-resolved fluorescence measurements, 4 mm × 10 mm quartz cuvettes were used because of the relatively strong absorption of the HSA/AC conjugate thus ensuring the proper position of the illuminated sample area in the sample holder compartment. The influence of secondary fluorescence on the fluorescence lifetime was negligible at the concentration and sample thickness used. It was checked by measuring fluorescence lifetimes at lower fluorophore concentrations. The excitation wavelength was 380 nm, and the emission was observed at a right angle position (90°). The temperature of the sample space was controlled by a thermostatic bath.

2.3. Data analysis

In this section the key expressions are summarized. Further details of the calculations can be found in Buzády et al. [14].

The time evolution of the fluorescence emission spectrum due to dielectric relaxation is characterized by the Stokes shift response function $S(t)$:

$$S(t) = \frac{\bar{\nu}(t) - \bar{\nu}(\infty)}{\bar{\nu}(0) - \bar{\nu}(\infty)}, \tag{1}$$

where

$$\bar{\nu}(t) = \frac{\int I(\nu,t)\nu \mathrm{d}\nu}{\int I(\nu,t)\mathrm{d}\nu} \tag{2}$$

is the first moment of the emission spectrum at some time. $I(\nu,t)$ stands for the fluorescence intensity at wavenumber ν and time t. $\bar{\nu}(t)$ is the mean wavenumber of the spectrum.

The emission spectra are measured at equidistant points in the wavelength space, thus the first moment should be calculated as:

$$\bar{\nu}(t) = \frac{\int I(\lambda,t)\lambda^{-3}\mathrm{d}\lambda}{\int I(\lambda,t)\lambda^{-2}\mathrm{d}\lambda}, \tag{3}$$

where $I(\lambda,t)$ stands for the fluorescence intensity at wavelength λ and time t. The temporal evolution of the dielectric relaxation was calculated by fitting $\bar{\nu}(t)$ and not $S(t)$, thus neglecting the need

of assumptions for the unknown value of $\nu(\infty)$:

$$\begin{aligned}\bar{\nu}(t) &= \bar{\nu}(\infty) + [\bar{\nu}(0) - \bar{\nu}(\infty)]S(t) \\ &= \bar{\nu}(\infty) + [\bar{\nu}(0) - \bar{\nu}(\infty)]\sum_i a_i e^{-t/\tau_{DRi}} \\ &= \bar{\nu}(\infty) + \sum_i b_i e^{-t/\tau_{DRi}} \quad . \end{aligned} \tag{4}$$

where τ_{DRi} stands for the lifetime components of dielectric relaxation, a_i stand for the preexponentials in $S(t)$ and b_i stand for the preexponentials in $\bar{\nu}(t)$. From Eq. (4) it is obvious that

$$\frac{a_i}{a_j} = \frac{b_i}{b_j}. \tag{5}$$

The spectral width of the emission spectrum is characterized by the square root of the ratio of the second-order central moment and the zero-order moment of the spectrum:

$$\Delta\nu(t) = \left(\frac{\int I(\nu,t)[\nu - \bar{\nu}(t)]^2 \mathrm{d}\nu}{\int I(\nu,t)\mathrm{d}\nu} \right)^{1/2} \quad . \tag{6}$$

This definition of spectral width differs from the other widely used parameter: the full width at half maximum (FWHM). In the case of AC $\Delta\nu(t) \approx 2.7$ FWHM.

The $\bar{\tau}$ average lifetime is also an illustrative parameter characterizing the fluorescence emission at different wavelengths:

$$\bar{\tau}(\nu) = \frac{\int I(\nu,t)t\mathrm{d}t}{\int I(\nu,t)\mathrm{d}t}. \tag{7}$$

When the fluorescence decay is to be written in terms of exponentials, $\bar{\tau}$ can be calculated as:

$$\bar{\tau}(\nu) = \frac{\sum_i a_i \tau_i^2}{\sum_i a_i \tau_i}. \tag{8}$$

3. Results

3.1. Steady-state spectra

The emission spectrum of HSA/AC is temperature dependent. At lower temperatures the spectra are blue-shifted (Fig. 2) compared to those measured at higher temperature. The spectral position depends less on the temperature than was observed in the emission of the Trp group [14]. The shape of the spectrum does not vary in the temperature range studied.

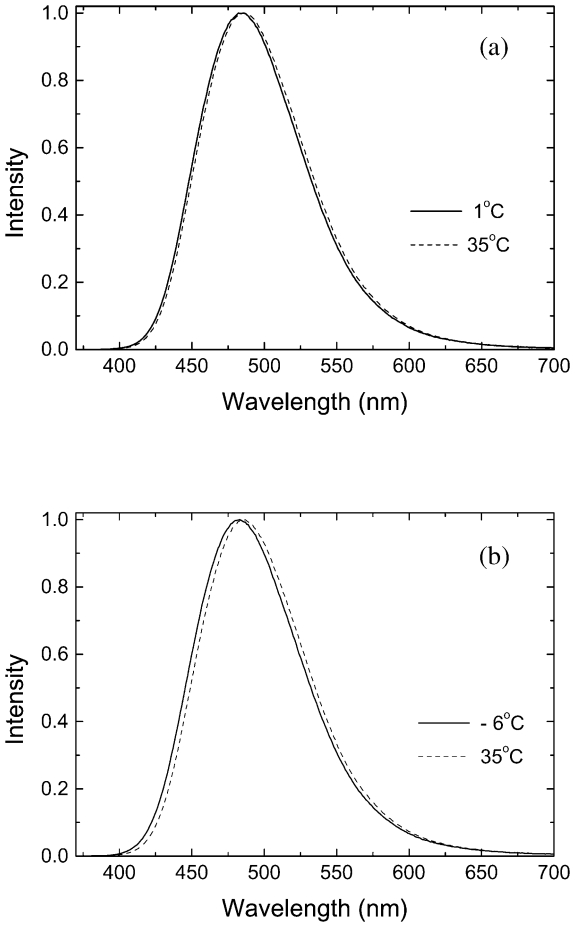

Fig. 2. Normalized emission spectra. (a) HSA/AC in buffer, (b) HSA/AC in glycerol/buffer. $\lambda_{ex} = 380$ nm (see also Section 2.1 and Section 2.2).

3.2. Time-resolved measurements

Time-resolved measurements were made by phase-fluorometry. Fluorescence decays were measured between 420 and 560 nm at 15 equidistant wavelength positions. The shape of the fluo-

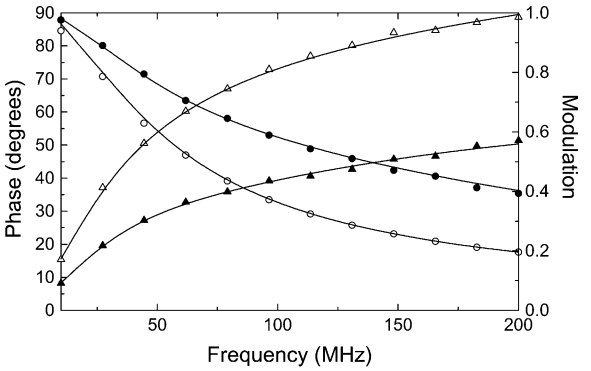

Fig. 3. Typical phase and modulation data measured at the blue side (420 nm, full signs) and the red side (560 nm, open signs) of the emission spectrum. Phase data: up triangles, modulation data: circles. HSA/AC in buffer, $\lambda_{ex} = 380$ nm, $T = 22$°C.

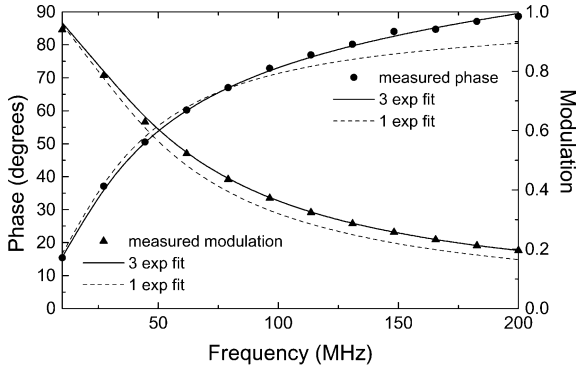

Fig. 4. Measured and calculated phase and modulation data at the red side of the emission spectrum. HSA/AC in buffer, $\lambda_{ex} = 380$ nm, $\lambda_{ex} = 560$ nm, $T = 22$°C.

rescence decay changes through stepping from the blue side towards the red side of the spectrum. Fig. 3 shows representative measured phase and modulation data at the two extremes of the wavelength range studied. It can be seen that the fluorescence decay at the red side of the spectrum is much slower than it is at the blue side.

In Fig. 4 different fits for phase-fluorometry data of a red side fluorescence decay are plotted. The monoexponential fit is quite poor. Satisfying fit can be reached using three exponentials, one of them describes the extremely fast component and two others are needed for fitting the slower components. Using more than three exponentials does not give noticeable improvement compared to the three-exponential fit.

From phase and modulation data the decay curves of fluorescence emission were constructed using three exponentials. Fig. 5 displays the shape of fluorescence decays at the blue side, at the maximum and at the red side of the emission spectrum. The decay is fastest at the blue side and slowest at the red side. The apparent fluo-

Table 1
Typical apparent fluorescence lifetimes

λ_{em} (nm)	a_1	a_2	a_3	τ_1 (ns)	τ_2 (ns)	τ_3 (ns)
420	0.52	0.42	0.06	3.81	0.95	0.01
430	0.61	0.35	0.04	3.76	1.05	0.01
440	0.70	0.26	0.04	3.71	1.17	0.01
450	0.76	0.22	0.02	3.84	1.20	0.01
460	0.86	0.14	–	3.76	0.94	–
470	0.93	0.07	–	3.76	0.78	–
480	0.91	0.08	–	4.00	1.31	–
490	0.85	0.15	–	4.18	2.25	–
500	0.88	0.13	−0.01	4.29	2.02	0.01
510	0.90	0.12	−0.02	4.30	2.46	0.01
520	0.90	0.12	−0.02	4.31	2.75	0.01
530	0.93	0.09	−0.02	4.36	2.21	0.01
540	0.93	0.09	−0.02	4.38	2.34	0.01
550	0.95	0.09	−0.04	4.44	1.99	0.01
560	0.95	0.09	−0.04	4.45	1.99	0.01

Three-component fits, HSA/AC in buffer, $\lambda_{ex} = 380$ nm, $T = 22$°C. The error of lifetime data is ± 0.03 ns.

rescence lifetime components are summarized in Table 1. Note the rising part of the red side-decay curve. At wavelengths shorter than the emission maximum (λ_{max}) all of the preexponentials have positive values. For longer wavelengths, the lifetime components became longer and/or the preexponential of the longest lifetime component becomes higher than that value of the medium lifetime component. At the red side of the spectrum the shortest fluorescence lifetime component has a negative preexponential. Among the three apparent fluorescence lifetime components the shortest one has a value of 10 ps. In the evaluation process it was fixed. This means that there is a very fast fluorescence lifetime component, which cannot be exactly resolved by our measurements. The relative weight (i.e. the preexponential) of this fast component can be calculated correctly, but the real value of this lifetime component cannot be resolved.

The negative preexponential at the red side of the spectrum shows unambiguously the presence of the excited state reaction, namely that of the DR. The same conclusion can be reached by performing another, rarely cited calculation. From measured modulation (m) and phase (Φ) data an $m/\cos\Phi$ value can be calculated [28,29]. If this value is higher than 1, it means that a negative preexponential can be found when fitting with a series of exponentials. Usually this $m/\cos\Phi$ parameter is displayed vs. the emission wavelength using data measured at a fixed modulation frequency. Fig. 6 shows a much more complete dataset. For a given sample at a fixed temperature all of the phase and modulation data measured at different emission wavelengths and different frequencies (14×12 m and Φ pairs) were used to construct the frequency–wavelength matrix (FWM) displayed as a contour plot of $m/\cos\Phi$ data. $m/\cos\Phi < 1$ is at the blue side of the spectrum ($\lambda < \lambda_{max}$) and $m/\cos\Phi > 1$ is at the red side of the spectrum ($\lambda > \lambda_{max}$). The full dataset of FWM clearly demonstrates the presence of DR. The dataset shown is a representative one. In the case of buffer solution and at different temperatures the picture looks similar.

From the fluorescence decays the mean emission wavenumber, $\bar{\nu}(t)$ (frequently called center-

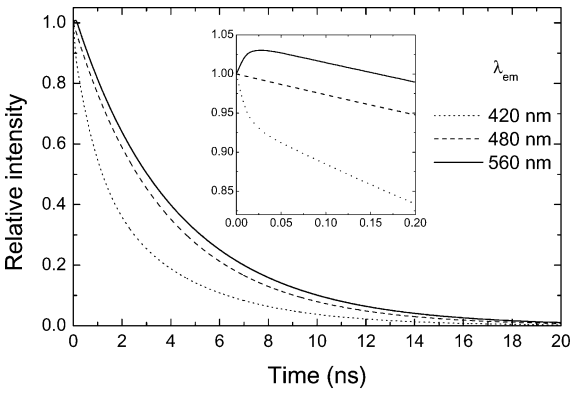

Fig. 5. Fluorescence decays of HSA/AC in buffer, including an expanded view of the initial rise at short time. $\lambda_{ex} = 380$ nm, $T = 22$°C.

of-gravity of the spectrum) was calculated (see Section 2.3). Fig. 7 shows the $\bar{\nu}(t)$ functions. The relevant part of the DR's decay is plotted. At longer times, when the fluorescence intensity becomes very low, the small differences in the longer lifetime components of the fittings of fluorescence decays will dominate and the move of $\bar{\nu}(t)$ intensity in time could show artifacts.

The following can be concluded from Fig. 7:

- For the first time (< 20 ps) there is a fast red-shift. For its characteristic time an upper limit value (10 ps) can only be derived from our measurements.
- In the sub-nanosecond and nanosecond time region the DR has clearly a non-monoexponential behavior. This longer time scale evolution of DR can be fitted satisfactorily with two further DR decay components. It means that DR decay of HSA/AC can be described well using three exponentials. A three-exponential fit and residuum function are plotted in Fig. 8. It should be pointed out, that — especially when the DR decay components do not differ by orders of magnitude — very similar decay shapes can be constructed using a few discrete exponentials or with wider distribution of lifetime components or even with a stretched exponential. From our data it can be concluded that there is an extremely

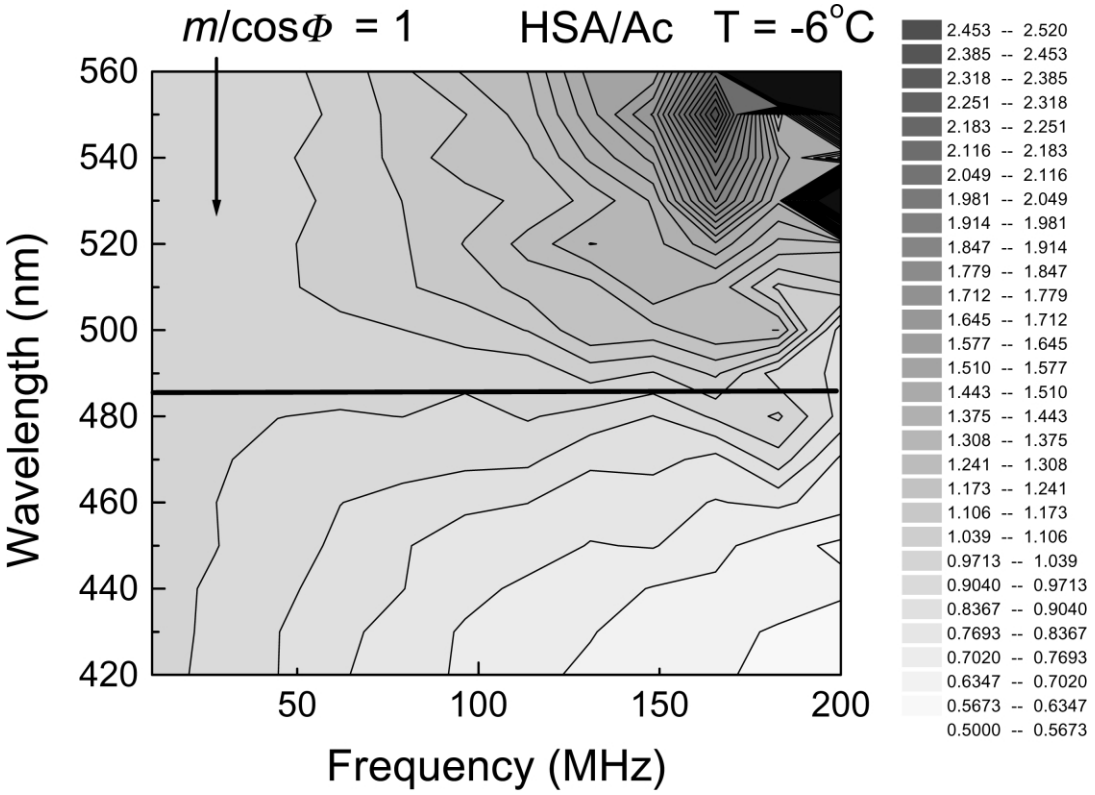

Fig. 6. Contour plot of $m/\cos\Phi$ as a function of frequency and wavelength. HSA/AC in glycerol/buffer. The black horizontal line highlights the wavelength position of emission maximum (λ_{max}). $T = -6$°C.

fast relaxation after the photoexcitation. The later part of DR should be characterized with a distributed DR decay behavior — which, of course, can be fitted in different ways. Characteristically, the long-time DR has lifetime components between 0.9 and 14 ns. Among them, the faster DR decay component is between 900 and 1400 ps, and the longer one is between 6 and 14 ns. These two components appear in each DR decay indicating two major steps in dielectric relaxation of HSA around AC. This may reflect the role of both the neighboring amino acid groups and the more distant protein environments in the DR. The fitting results of DR decays are summarized in Table 2.

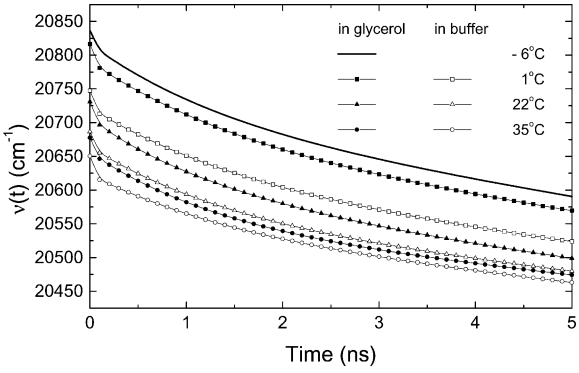

Fig. 7. Time evolution of $\bar{\nu}(t)$ mean fluorescence wavenumbers at different temperatures. HSA/AC in glycerol/buffer, HSA/AC in buffer. $\lambda_{ex} = 380$ nm.

- The shape of DR decays do not practically change with temperature in the temperature range studied. This means that DR around AC probe reflects motions of the protein environment which are less affected by the temperature.

Table 2
Decay parameters of DR

Temperature (°C)		y_0 (cm^{-1})	a_1	a_2	a_3	t_1 (ns)	t_2 (ns)	t_3 (ns)
35	Buffer	20 262	27.3	74.2	287.0	0.01	1.39	13.72
	Glycerol	20 350	21.2	89.5	217.6	0.01	1.17	8.90
22	Buffer	20 346	22.0	78.5	240.4	0.01	1.20	8.50
	Glycerol	20 375	23.9	60.6	271.5	0.01	0.91	6.40
1	Buffer	20 327	25.1	89.2	305.6	0.01	1.43	10.99
	Glycerol	20 410	25.4	73.4	307.5	0.01	1.21	7.55
−6	Glycerol	20 437	19.3	62.2	318.2	0.01	0.96	6.89

$\bar{\nu}(t) = y_0 + a_1 \exp(-t/t_1) + a_2 \exp(-t/t_2) + a_3 \exp(-t/t_3)$.

- A small but significant difference can be observed between the initial values of $\bar{\nu}(t)$ functions (Fig. 7). Although the concentration of glycerol in the solvent is not more than 10%, the fluorescence emission is slightly blue shifted in the presence of glycerol. In Fig. 7, $\bar{\nu}(t)$ wavenumber values of glycerol containing solutions are always higher than those of solutions without glycerol measured at the same temperature. This means that the presence of glycerol — at even this low concentration — affects the environment of AC. Cys-34 is not an entirely buried part of HSA, thus AC can effectively feel the polarity of the solvent. In the presence of glycerol the polarity of the solvent is lower, thus the fluorescence emission occurs at higher energies (i.e. at higher wavenumbers).
- Besides decreasing the polarity of the solvent, there is another consequence of the presence of glycerol. As can be seen from the data in Table 3, the fluorescence lifetime components of the total fluorescence of AC are shorter and/or the shorter component has higher weight in the presence of glycerol. The higher rate of non-radiative relaxation may have two origins. First, in the presence of glycerol the rate of collisional quenching of AC emission by solvent molecules may be higher. Second, to minimize the chemical potential, the protein environment around AC — similarly to the whole HSA molecule — reduces its surface area by adopting a more compact conformations and perturbed hydration layer. Earlier, the same fluorescence lifetime shortening was found when measuring the emission of the Trp group of HSA [14]. On the basis of present data the influence of these effects can not be distinguished.

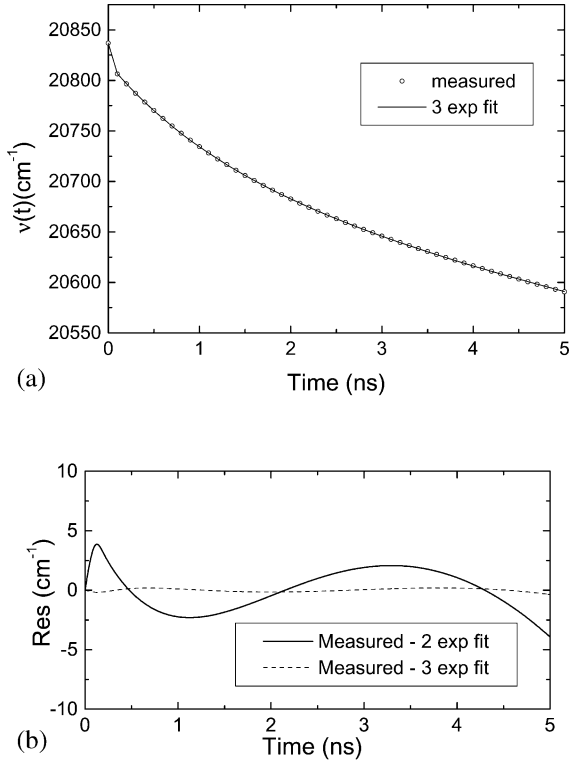

Fig. 8. Example for fits of $\bar{\nu}(t)$. Decay function and residuals. HSA/AC in glycerol/buffer. $\lambda_{ex} = 380$ nm, $T = -6$°C.

Finally, let us examine the temporal evolution of the $\Delta\nu(t)$ spectral width of AC's fluorescence

Table 3
Total fluorescence lifetime of HSA/AC

Temperature (°C)		a_1	a_2	τ_1 (ns)	τ_2 (ns)	$\bar{\tau}$ (ns)
35	Glycerol	0.17	0.83	1.37	3.90	3.73
	Buffer	0.13	0.87	1.28	3.97	3.85
22	Glycerol	0.15	0.85	1.46	4.06	3.90
	Buffer	0.11	0.89	1.33	4.07	3.97
1	Glycerol	0.19	0.81	1.90	4.34	4.11
	Buffer	0.14	0.86	1.72	4.36	4.20
−6	Glycerol	0.26	0.74	2.64	4.46	4.15

$\lambda_{ex} = 380$ nm. The error of lifetime data is ± 0.03 ns. Total fluorescence curves were constructed with summarizing the separate fluorescence decay curves of different wavelength using the proper spectral weights.

emission (Fig. 9). $\Delta\nu(t)$ was calculated according to Eq. (6).

- At the very beginning of $\Delta\nu(t)$ curves a small, fast change can be seen.
- After the first few tens of picoseconds, a slight, but continuous decreasing of spectral width is observed. $\Delta\nu(t)$ decreases approximately 1 nm after 5 ns. (It is equal to an approx. 2.7 nm decrease of FWHM.) Two statements can be made. First, decreasing of $\Delta\nu(t)$ — similarly to the temporal change of $\bar{\nu}(t)$ — reflects a practically temperature-independent evolution shape in time. Second, $\Delta\nu(t)$ has — by a little, but significantly — higher values (i.e. the spectrum is wider) at lower temperatures and in the presence of glycerol. This means that the fluorescence emission starts from a relatively wider-distributed excited state manifold. After time, the excited state AC probe groups become relaxed thus the emission is produced from a narrower excited state energy band.

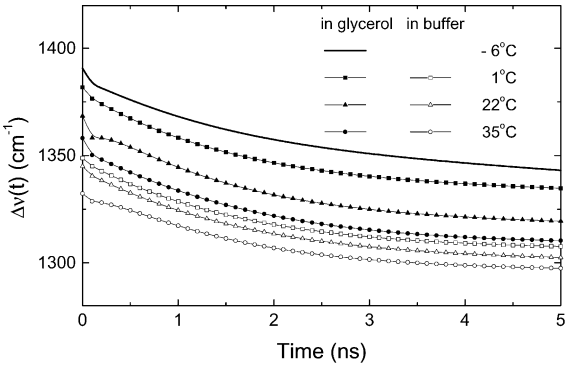

Fig. 9. Time evolution of $\Delta\bar{\nu}(t)$ spectral width at different temperatures. HSA/AC in glycerol/buffer, HSA/AC in buffer. $\lambda_{ex} = 380$ nm.

4. Conclusions

A strong non-exponentiality of fluorescence decay of AC-labeled HSA was observed. The study of fluorescence emission of the fluorescence probe shows the presence of DR unambiguously. It is supported by the presence of negative preexponentials in the terms of exponential series describing the fluorescence decay at the red side of the emission spectrum. After the photoexcitation a fast (< 10 ps) DR component appears. Later a slower DR decay can be observed which is characterized by distributed DR-lifetime behavior. Typically, the DR decay ranges between 0.4 and 10 ns.

In the presence of glycerol (10% w/w) the total fluorescence decay of AC is a bit faster but the DR has practically the same decay characteristics. It is concluded that the higher rate of non-radiative processes of AC is a consequence of the higher rate of collisional quenching in the presence of glycerol.

The average total fluorescence lifetime becomes lower in the presence of glycerol, but the DR decay does not change. This means that this low concentration of glycerol does not cause dif-

ferences in the protein environment of the AC group.

Comparing the DR decays characteristics of AC and Trp groups in HSA in both cases a distributed behavior of DR decay around the fluorescence reporter group was detected. A significant difference is that in the case of AC a very fast (< 10 ps) DR component was found. On the sub-nanosecond and nanosecond time scale both of the systems show distributed DR decay characteristics. A two-component fit for the slower motions describe satisfactorily both of the systems.

The different DR decay components are attributed to the different scale and different frequency motions of HSA environment of AC.

Acknowledgements

This work was supported by grants from: Hungarian National Scientific Research Foundation No. T032700 and No. T034443.

References

[1] D.W. Pierce, S.G. Boxer, Dielectric relaxation in a protein matrix, J. Phys. Chem. A 96 (1992) 5560–5566.
[2] E. Laitinen, K. Salonen, T. Harju, Solvation dynamics of 4-amino-*N*-methyl-phthalimide in *n*-alcohol solutions, J. Chem. Phys. 104 (1996) 6138–6148.
[3] E. Laitinen, K. Salonen, T. Harju, Solvation dynamics of 3-aminophthalimide in *n*-butanol solution at different temperatures, J. Chem. Phys. 105 (1996) 9771–9780.
[4] C.P. Hsu, Y. Georgievskii, R.A. Marcus, Time-dependent fluorescence spectra of large molecules in polar solvents, J. Phys. Chem. A 102 (16) (1998) 2658–2666.
[5] Z. Wasylewski, H. Koloczek, A. Wasniowska, K. Slizowska, Red-edge excitation fluorescence measurements of several two-tryptophan-containing proteins, Eur. J. Biochem. 206 (1992) 235–242.
[6] R. Vos, Y. Engelborghs, J. Izard, D. Baty, Fluorescence study of the three tryptophan residues of the pore-forming domain of Colicin A using multifrequency phase fluorometry, Biochemistry 34 (1995) 1734–1743.
[7] A.P. Demchenko, I. Gryczynski, Z. Gryczynski, W. Wiczk, H. Malak, M. Fishman, Intramolecular dynamics in the environment of the single tryptophan residue in staphylococcal nuclease, Biophys. Chem. 48 (1993) 39–48.
[8] M. Eftink, Quenching-resolved emission anisotropy studies with single and multitryptophan-containing proteins, Biophys. J. 43 (1983) 323–334.
[9] K.J. Willis, A.G. Szabo, M. Zukker, J.M. Ridgeway, B. Alpert, Fluorescence decay kinetics of the tryptophyl residues of myoglobin: effect of heme ligation and evidence for discrete lifetime components, Biochemistry 29 (1990) 5270–5275.
[10] M. Vincent, J. Gallay, A.P. Demchenko, Dipolar relaxation around indole as evidenced by fluorescence lifetime distributions and time-dependence spectral shifts, J. Fluorescence 7 (1) (1997) 107S–110.
[11] J.R. Lakowicz, H. Cherek, Dipolar relaxation in proteins on the nanosecond timescale observed by wavelength-resolved phase fluorometry of tryptophan fluorescence, J. Biol. Chem. 255 (3) (1980) 831–834.
[12] A.P. Demchenko, J. Gallay, M. Vincent, H.J. Apell, Fluorescence heterogeneity of tryptophans in Na,K-ATPase: evidences for temperature-dependent energy transfer, Biophys. Chem. 72 (1998) 265–283.
[13] M. Vincent, A.M. Gilles, I.M. Li de la Sierra, P Briozzo, O. Barzu, J. Gallay, Nanosecond fluorescence dynamic Stokes shift of Tryptophan in a protein matrix, J. Phys. Chem. 104 (47) (2000) 11286–11295.
[14] A. Buzády, J. Erostyák, B. Somogyi, Phase-fluorimetry study on dielectric relaxation of human serum albumin, Biophys. Chem. 88 (2000) 153–163.
[15] A. Sytnik, I. Litvinyuk, Energy transfer to a proton-transfer fluorescence probe: Tryptophan to a flavonol in human serum albumin, Proc. Natl. Acad. Sci. USA 93 (1996) 12959–12963.
[16] M. Lasagna, V. Vargas, D.M. Jameson, J.E. Brunet, Spectral properties of environmentally sensitive probes associated with horseradish peroxidase, Biochemistry 35 (1996) 973–979.
[17] R. Wang, F.V. Bright, Rotational reorientation kinetics of dansylated bovine serum albumin, J. Phys. Chem. 97 (1993) 4231–4238.
[18] F. Moreno, M. Cortijo, J. Gonzalez-Jimenez, The fluorescent probe prodan characterizes the warfarin binding site on human serum albumin, Photochem. Photobiol. 69 (1) (1999) 8–15.
[19] X.M. He, D.C. Carter, Atomic structure and chemistry of human serum albumin, Nature 358 (1992) 209–215.
[20] F.G. Prendergast, M. Meyer, G.L. Carlson, S. Iida, J.D. Potter, Synthesis, spectral properties and use of 6-acryloyl-2-dimethylaminonaphtalene (Acrylodan), J. Biol. Chem. 258 (12) (1983) 7541–7544.
[21] J.D. Jordan, R.A. Dunbar, F.V. Bright, Dynamics of acrylodan-labeled bovine and human serum albumin entrapped in a sol–gel-derived biogel, Anal. Chem. 67 (1995) 2436–2443.
[22] J.S. Lundgren, M.P. Heitz, F.V. Bright, Dynamics of acrylodan-labeled bovine and human serum albumin sequestered within aerosol-OT reverse micelles, Anal. Chem. 67 (1995) 3775–3781.
[23] R. Wang, S. Sun, E.J. Bekos, F.V. Bright, Dynamics surrounding Cys-34 in native, chemically denaturated and silica-adsorbed bovine serum albumin, Anal. Chem. 67 (1995) 149–159.

[24] C.M. Ingersoll, J.D. Jordan, F.V. Bright, Accessibility of the fluorescent reporter group in native, silica-adsorbed, and covalently attached acrylodan-labeled serum albumins, Anal. Chem. 68 (1996) 3194–3198.
[25] R. Narazaki, T. Maruyama, M. Otagiri, Probing the cystein 34 residue in human serum albumin using fluorescence techniques, Biochim. Biophys. Acta 1338 (1997) 275–281.
[26] K. Flora, J.D. Brennan, G.A. Baker, M.A. Doody, F.V. Bright, Unfolding of acrylodan-labeled human serum albumin probed by steady-state and time-resolved fluorescence methods, Biophys. J. 75 (1998) 1084–1096.
[27] M.D. Garrison, D.J. Iuliano, S.S. Saavedra, G.A. Truskei, W.M. Reichert, Post adsorption changes in the emission maximum of acrylodan-labeled bovine serum albumin using total internal reflection fluorescence, J. Colloid Interface Sci. 148 (1992) 415–424.
[28] T.V. Veselova, L.A. Limareva, A.S. Cherkasov, V.I. Shirokov, Fluorometric study of effect of solvent on the fluorescence spectrum of 3-amino-*N*-methylphthalimide, Opt. Spectrosc. 19 (1965) 39–43.
[29] J.R. Lakowicz, A. Balter, Theory of phase-modulation fluorescence spectroscopy for excited state processes, Biophys. Chem. 16 (1982) 99–115.